Magnetic Manifestations of Carrier Confinement in Quantum Wells

D. D. Awschalom, J. Warnock, J. M. Hong, L. L. Chang, M. B. Ketchen, and W. J. Gallagher
IBM Watson Research Center, P.O. Box 218, Yorktown Heights, New York 10598
(Received 9 November 1988)

A combination of superconducting integrated circuits was used to construct a very sensitive magneto-optic microsusceptometer for observations of the optically induced magnetization in $Cd_{1-x}Mn_xTe$ multiple quantum wells. Spin-polarized electrons and holes are created optically, and the quantum mechanically localized wave functions of the carriers then serve as microscopic probes of the magnetic behavior. Both the magnitude and the picosecond dynamics of the magnetic response have been studied and reveal the effects of carrier quantization.

PACS numbers: 75.50.Rr, 73.20.Dx, 75.50.Pp, 78.20.Ls

It has been well established that quantum size effects play an important role in modifying the electrical and optical properties of microscopic systems. In particular, with the development of molecular-beam epitaxy as a technique for growing high-quality superlattice structures with monolayer control, detailed studies of quantum confinement effects have become possible, revealing a wide variety of interesting and often puzzling phenomena. Lately, it has been shown that diluted magnetic semiconductors[1] (DMS) can be incorporated into such superlattice structures,[2,3] offering the possibility of changing the confining potential by the application of an external magnetic field. A similar opportunity exists to study the effects of carrier confinement on the magnetic and magneto-optical properties of a quantum system. Although the optical and electronic properties of DMS superlattices have been studied in some detail,[1,4,5] direct magnetic studies are considerably more difficult, and only a few such experiments have been reported.[6,7] It would also be interesting to probe the magnetic behavior on a *local* scale by exploiting the strong spin-spin interaction between the carriers and the magnetic ions. In a quantum-well structure, spin-polarized carriers can induce a magnetization whose spatial extent will be completely determined by the quantum-mechanical wave functions of the confined carriers. Therefore, with DMS superlattices, one may construct a tailored potential to shape the electronic wave functions and vary the length scale of the magnetic probe, thereby providing an opportunity to study quantum phenomena in a new way.

In this paper we report a direct study of the optically induced magnetism in a semiconductor quantum-well system, aimed at exploring the connection between the electronic and magnetic properties of these heterostructures. This magnetism is induced by optically generated carriers through a local spin-spin exchange interaction with the magnetic moments, so that the region of magnetization matches the extent of the carrier wave functions. Thus the magnetic behavior of the structure can be probed by exploiting the quantum-mechanical nature of the localized carrier and varying the penetration of the excitonic wave function into the nearby barriers. This can be effectively accomplished by changing the width of the potential well or by exciting carriers into higher quantum levels, where the wave-function penetration grows with increasing energy. The experiments employed $Cd_{1-x}Mn_xTe$-$Cd_{1-y}Mn_yTe$ superlattice structures which were excited optically by picosecond pulses. The magnetization was detected with an ultra-low-noise dc-SQUID–based microsusceptometer, configured to operate near the quantum limit of sensitivity. Time-averaged magnetic spectroscopy measurements were performed, revealing the connection between the quantum confinement of the electrons and holes and the magnetic properties through the appearance of well-defined structure in the spectra. Unlike the electronic dynamics, the time-resolved behavior of this magnetization was found to be critically dependent on the width of the quantum well and the energy of the confined carriers.

Multiple quantum wells were fabricated by use of periodic layers of magnetic $Cd_{1-x}Mn_xTe$ having alternating Mn^{2+} concentrations, x. These (111)-oriented superlattice structures were grown by molecular-beam epitaxy on (100) GaAs substrates, after deposition of a CdTe buffer of $\sim$1500 Å. The composition alternated between $x=0.065$ (1.71-eV band gap) for the wells and $x=0.38$ (2.21-eV band gap) for the barriers. The barrier widths were fixed at 84 Å and the well widths varied from 84 to 21 Å. In addition, the number of periods for any given sample was set in inverse proportion to the well thickness, so that the total deposited thickness of the well material was the same for all samples. Both well and barrier layers were thin enough so that the lattice mismatch could be accommodated by elastic strain,[8] and the defect density in the layers was thus minimal. The integrity of these superlattices was determined from x-ray diffraction and photoluminescence studies.[9] After fabrication of a superlattice, the GaAs substrate was thinned and the structure cleaved into $\sim$200-μm squares. The optical excitation was in the form of picosecond pulses from a tunable dye-laser source, synchronously pumped by a mode-locked Nd-doped yttrium

aluminum garnet laser, frequency doubled to 532 nm at a 76-MHz repetition rate. The laser light was circularly polarized, then focused into a single-mode polarization-preserving optical fiber, and guided to the sample which was mounted in the microsusceptometer.

Three distinct superconducting integrated circuits were interconnected to form the nearly quantum-limited microsusceptometer. A miniature pickup loop was fabricated on a transparent quartz substrate, allowing light to be directly incident on the superlattice structure while maintaining close physical contact between the superlattice epilayers and the pickup loop. In order to reduce the effects of stray magnetic fields, the pickup loop structure consisted of two superconducting, square counterwound loops, 25 μm on a side, one of which was in close contact with the sample. The terminals of this gradiometer loop assembly were connected with short superconducting aluminum wire bonds to the five-turn input coil of an integrated planar dc SQUID. In order to reduce the noise from room-temperature electronics,[10] this detector SQUID was operated open loop in a small-signal amplifier mode and read out in turn by a second dc SQUID operating in a conventional flux-locked loop circuit. The SQUID's and miniature pickup coils were fabricated with a Josephson integrated circuit process developed for research applications.[11] Details of the microsusceptometer fabrication, characterization, and calibration are given elsewhere,[12] where it has been shown that the detector noise is nearly quantum limited, with a magnetic flux noise of $\phi_n = 8.4\times10^{-8}\phi_0/\mathrm{Hz}^{1/2}$ in the white-noise region at $T = 290.0$ mK. This corresponds to an energy sensitivity[13] of about $1.7\hbar$ at 1 kHz. A sample is placed superlattice side down upon one of the pickup loops and the experimental system cooled to ^{3}He temperatures in an rf-tight box with superconducting electronics. For the time-averaged measurements, the magnetic response of the quantum-well sample is monitored as a function of the photon energy of the incident radiation. A pump-probe technique is used[14] for the time-resolved measurements, with the microsusceptometer serving as an integrating magnetic detector in a boxcar averaging scheme. A transient magnetization is induced in the sample by the pump pulse, and the magnetic response of the system is probed at a time δt later by a much weaker probe pulse. The system's response to the probe pulse will depend on the pump-induced magnetization of the sample,[15] so that the rise and subsequent decay of the pump-induced magnetization can be mapped out by systematically varying the delay time between the pump and probe pulses. This procedure can be repeated in a signal averaging mode, a typical series of scans requiring about 12 h to complete.

The time-averaged magnetic data are shown in Fig. 1 for quantum wells of three different widths, where the magnetization of the sample is plotted as a function of the photon energy of the exciting radiation. Several interesting features are immediately apparent. The magnetic response is noticeably altered by quantum-size affects, leading to clear peaks in the magnetic signal. This is a direct manifestation of excitonic confinement in the magnetic response of the system, and consistent with the appearance of quantized states. In the 84-Å wells [Fig. 1(a)], the effect of the predicted quantum levels is clearly seen, with definite peaks in the response seen at about 1.75, 1.88, and a weaker feature at about 1.98 eV. These features are seen at approximately the energies expected for the excitons associated with the $n=1$, $n=2$, and $n=3$ confinement subbands, based on the predictions of a simple Kronig-Penney–type calculation with a small valence-band offset. While pumping at intermediate energies (i.e., between two of the subbands), the magnetic signal does not fall to zero, but rather stays at some relatively constant level. This part of the signal can be attributed to band-to-band transitions, which form a continuum since the carriers are not laterally confined. The spin-polarized carriers very quickly ($\sim$1 ps) transfer their polarization to the sea of magnetic ions through spin-flip exchange scattering events,[16] resulting in an induced magnetization which is relatively independent of the carrier energy. The onset of the magnetic signal occurs slightly below the exciton energy, presumably as a result of transitions from acceptor levels to the conduction band or shallow donor states.[17] This transition moves to higher energy as the electronic levels are shifted by confinement effects. This trend is illustrated by the data from the 42-Å wells [Fig. 1(b)], where the threshold of the magnetic response moves to a relatively higher energy, the spacing between confinement sub-

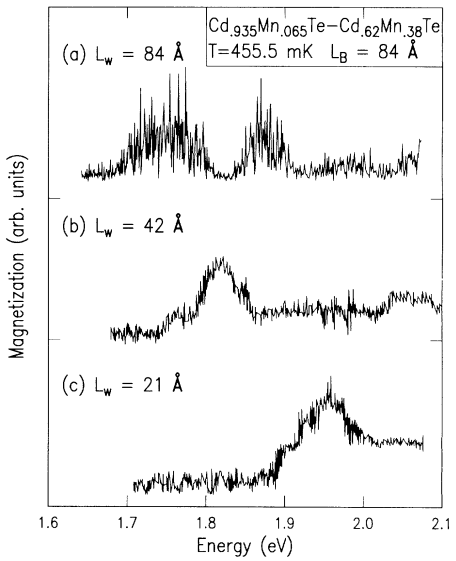

FIG. 1. Magnetic spectroscopy of three quantum-well superlattices with fixed barrier width L_b and varying well width L_w. The total number of periods are (a) 30, (b) 60, and (c) 120, respectively. The y tickmarks indicate the relative zeros of magnetization.

bands is widened, and the number of subbands is reduced. The two predicted quantum levels are seen at 1.82 and 2.05 eV, respectively. Finally, in the narrowest wells studied only one confinement level is expected in the conduction band, and this single level is indeed observed at 1.96 eV [Fig. 1(c)].

The dynamical response of the magnetic state resulting from the injection of spin-polarized carriers was measured by use of picosecond transient magnetic spectroscopy. It should be emphasized that this experiment measures local relaxation times, where individual spins have been oriented via a strong local field or through a spin-flip exchange interaction. Macroscopic reorientation processes may involve the realignment of complex, interlinked chains of spins (as in a spin-glass, for example), where relaxation times or frequency dependences are much more difficult to predict. Figure 2 shows the time-resolved data from the 84-Å wells, taken with the excitation energy successively tuned to the $n=1$, $n=2$, and $n=3$ quantum levels. The magnetic-relaxation lifetime is observed to decrease dramatically as the excitation energy is increased. Phenomenologically, it is well known that the local-magnetic-relaxation time decreases substantially as the magnetic dilution is increased,[14,18] and one can obtain[14] rough estimates of 3 ns for the relaxation time in the wells ($x=0.065$) and 20 ps for the relaxation time in the barriers ($x=0.38$). For excitonic states, where the electrons and holes are mainly confined to the wells and the wave functions do not penetrate the barrier significantly, the relaxation time is thus expected to be rather long. For the higher-energy states, where the penetration is more significant, a larger part of the induced magnetization signal is associated with reorientation of the spins in the barriers, and hence the average relaxation time is expected to be shorter. This is clearly seen in the data of Fig. 2. Since the magnetic concentration is much higher in the barriers than in the wells, the signal from the barriers will tend to dominate the overall effect as soon as the overlap of the wave function into the barriers becomes significant. This description would also predict that, for optical creation of carriers in the ground state, the relaxation time should decrease in the same sudden way as the confining-well width is decreased. The dynamical response for three different confining potentials is shown in Fig. 3, where the carrier energy is tuned to the $n=1$ resonance in each case. Indeed, the relaxation times decrease markedly with decreasing dimension. Thus, by changing either the carrier energy or the well width, the physical location of the induced magnetization signal can be controlled by the shape of the carrier wave function, so that the magnetic behavior of the quantum wells and barriers can be probed in a systematic way. It is interesting to note that the time scale of the magnetic response can be significantly longer and change much more rapidly than the carrier lifetime over this range of well widths. Independent luminescence measurements show a carrier lifetime ranging from 300

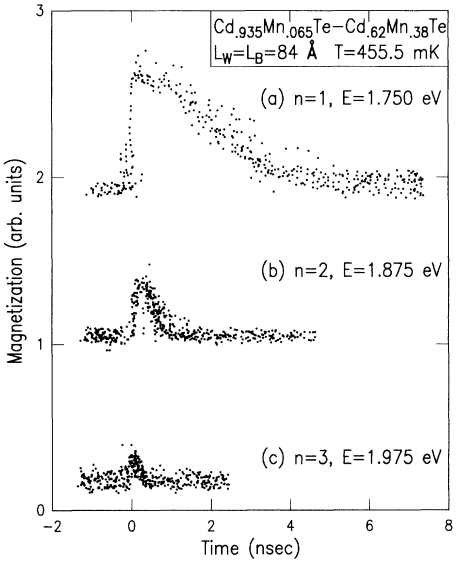

FIG. 2. Time-resolved magnetic spectroscopy for a superlattice of thirty periods with fixed well and barrier widths $L_w=L_b=84$ Å at various excitation energies. The energies correspond to the three magnetization peaks associated with the confinement subbands (a) $n=1$, (b) $n=2$, and (c) $n=3$ as observed in Fig. 1(a).

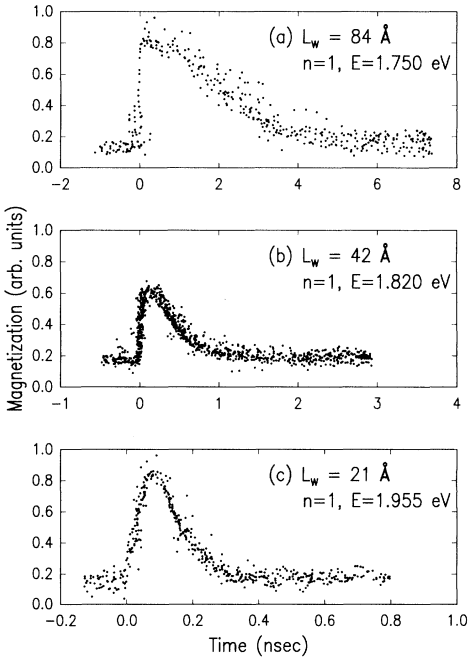

FIG. 3. Time-resolved magnetic spectroscopy for three $Cd_{0.935}Mn_{0.065}Te$-$Cd_{0.62}Mn_{0.38}Te$ superlattices at $T=455.5$ mK with fixed barrier width $L_b=84$ Å and varying well width L_w, on excitation at their respective $n=1$ levels. The number of periods are (a) 30, (b) 60, and (c) 120, respectively.

to 500 ps for these samples,[19] which is not much different from that in ordinary nonmagnetic GaAs quantum wells.[20] This implies that, for example, when tuning the excitation energy to the $n=1$ subband within the 84-Å wells, the quantized carriers impart a magnetic imprint on the system which evolves long after the carriers have recombined. If the excitation energy is increased, the magnetic-relaxation time decreases until this time becomes short relative to the carrier lifetime. The same effect is observed as the well width is decreased, confining the carriers, and forcing further wave-function penetration into the barriers. Therefore one may distinguish between electronic and magnetic effects by varying the quantum-well geometry.

In summary, studies of the magnetic dynamics in diluted magnetic semiconductor quantum-well structures have been reported for the first time, and direct observations were made of the effects of excitonic confinement on the magnetic behavior. The magnetic dynamics could be probed on a local scale with picosecond time resolution, with use of the quantum confined carriers to define the region of induced magnetization. By varying the confinement of the carriers, the penetration into the barriers and hence the physical location of the induced magnetization could be changed in a systematic way, providing not only information on the magnetic properties of the structure, but also information on the magnetic environment of the confined electrons and holes. Therefore, such local magnetic measurements provide a unique and powerful probe of carrier localization and magnetic interactions at quantum length scales.

We would like to thank J. Rozen and F. Agullo-Rueda for technical assistance, and A. Kleinsasser, R. L. Sandstrom, and B. Bumble for their fabrication expertise.

[1]O. Goede and W. Heimbrodt, Phys. Status Solidi (b) **146**, 11 (1988); W. Giriat and J. K. Furdyna, in *Semiconductors and Semimetals,* edited by J. K. Furdyna and J. Kossut (Academic, New York, 1988), Vol. 25, p. 1.

[2]R. N. Bicknell *et al.*, Appl. Phys. Lett. **45**, 92 (1984).

[3]L. A. Kolodziejski *et al.*, Appl. Phys. Lett. **45**, 440 (1984).

[4]X.-C. Zhang *et al.*, Phys. Rev. B **31**, 4056 (1985).

[5]J. Warnock *et al.*, Phys. Rev. B **32**, 8116 (1985).

[6]D. D. Awschalom *et al.*, Phys. Rev. Lett. **59**, 1733 (1987).

[7]J. Heremans and D. L. Partin, Phys. Rev. B **37**, 6311 (1988).

[8]L. A. Kolodziejski *et al.*, IEEE J. Quantum Electron. **22**, 1666 (1986).

[9]J. M. Hong *et al.*, J. Appl. Phys. **63**, 3285 (1988).

[10]M. B. Ketchen and C. C. Tsuei, in *SQUID '80,* edited by H.-D. H. Hahlbohm and H. Lubbig (de Gruyter, Berlin, 1980), p. 227.

[11]R. L. Sandstrom *et al.*, IEEE Trans. Magn. **23**, 1484 (1987).

[12]D. D. Awschalom *et al.*, Appl. Phys. Lett. **53**, 2108 (1988).

[13]J. Clarke, W. M. Goubau, and M. B. Ketchen, J. Low Temp. Phys. **25**, 99 (1976).

[14]D. D. Awschalom, J. Warnock, and S. von Molnar, Phys. Rev. Lett. **58**, 812 (1987).

[15]J. Warnock and D. D. Awschalom, Jpn. J. Appl. Phys. **26**, 819 (1987).

[16]H. Krenn, W. Zawadski, and G. Bauer, Phys. Rev. Lett. **55**, 1510 (1985).

[17]G. Neu *et al.*, J. Lumin. **21**, 293 (1980).

[18]E. A. Harris and K. S. Yngvesson, J. Phys. C **1**, 990 (1968).

[19]M. Freeman *et al.*, to be published.

[20]E. O. Gobel, J. Kuhl, and R. Hoger, J. Lumin. **30**, 541 (1985).